Hydrodynamics of electron-hole Coulomb drag

Yu. A. Pusep [1,*] M. A. T. Patricio [1] M. M. Glazov [2] G. M. Jacobsen [3] M. D. Teodoro [3] G. M. Gusev [4] and A. K. Bakarov [5]

[1] São Carlos Institute of Physics, University of São Paulo, IFSC-USP, 13566-590 São Carlos, São Paulo, Brazil
[2] Ioffe Institute, 194021 Saint Petersburg, Russia
[3] Physics Department, Federal University of São Carlos, 13565-905 São Carlos, São Paulo, Brazil
[4] Institute of Physics, University of São Paulo, 135960-170 São Paulo, São Paulo, Brazil
[5] Institute of Semiconductor Physics, 630090 Novosibirsk, Russia

(Received 19 May 2025; accepted 22 September 2025; published 16 October 2025)

A remarkable response of a three-component hydrodynamic plasma consisting of electrons, light holes, and heavy holes to an external electric field has been discovered in a quantum well structure where the field causes counterflows of light and heavy holes: Heavy holes propagate in the direction of the electric field, while light holes move in the direction opposite to the electric field, in the same direction as the electrons. The observed effect is due to the different scattering efficiencies of electrons by light and heavy holes, which causes the Coulomb drag of light holes by electrons, while the drift in the electric field is responsible for the propagation of heavy holes. As a consequence of the Coulomb electron-hole drag, negative conductivity of light holes is observed.

DOI: 10.1103/71yh-kprh

I. INTRODUCTION

Mutual electron-hole (e-h) Coulomb drag is a natural phenomenon for hydrodynamic e-h plasma, where interparticle momentum-conserving collisions dominate over random momentum-relaxing scattering [1]. It arises from the effective frictional forces caused by Coulomb interactions. Since the pioneering experiments [2,3], Coulomb drag has been widely studied in double-layer two-dimensional electron gas systems (see for review Ref. [4] and references therein), where electrons exhibiting the drag effect are spatially separated. At the same time, the Coulomb drag between electrons and holes that are not separated in space was discovered even earlier in Ge [5], Si [6], and GaAs/AlGaAs heterostructures [7]. In fact, the last two works were the first to discover the hydrodynamic properties of e-h plasma. A number of interesting phenomena arise in hydrodynamic electron systems due to the Coulomb drag, such as a negative absolute mobility [7–9] and a negative drag conductivity [10]. Moreover, the e-h drag influences the formation of plasma waves [11] and it causes spatial accumulation of charge and the accompanying sharp change in the optical properties [12]. The latter can be used to form high-density e-h plasma in semiconductor quantum wells (QWs).

So far, most of the research has focused on the influence of Coulomb drag on the electron transport properties. In fact, a common feature of e-h Coulomb drag effects is the decisive role of scattering-induced energy and momentum redistribution between electrons and holes, which is determined by their spatial distribution. Thus, the study of charge flows in the hydrodynamic e-h system helps to understand their specific motion.

The diffusion of holes photogenerated in a system of hydrodynamic two-dimensional electrons was studied in our recent paper [13], where the effect of e-h Coulomb drag was observed and qualitatively explained. However, the quantitative analysis of the data has not been performed and the question of why diffusion of holes is observed in an *n*-doped QW, where charge neutrality should be quickly achieved within the Maxwell relaxation time [14], remained open.

In this paper, the spatial distribution of charge carriers in the course of Coulomb drag is studied in detail and the results of an experimental study of the influence of Coulomb drag on the diffusion of holes optically injected into a hydrodynamic electron mesoscopic channel made of a high-mobility GaAs QW are presented. The spatial distribution of the injected holes is studied using a scanning photoluminescence (PL) microscopy setup. When an electric field is applied to the channel, the effect of electron drift on the spatial distribution of holes resulting in modification of their diffusion profile is observed. With increasing current, a strong asymmetry of the spatial diffusion profile is detected, caused by the drift of holes in the external electric field and their drag by the electron flow. It is shown that the injection of holes into a QW from barriers leads to the formation of a positive space charge in it, which is neutralized by the negative charge of electrons accumulated in the barriers. In this case, the relaxation of the

*Contact author: pusep@ifsc.usp.br

positive space charge occurs due to the diffusion of injected holes. The observed phenomenon is well explained by the standard drift-diffusion approach.

As mentioned above, similar Coulomb e-h drag and negative absolute mobility were observed in GaAs/AlGaAs multiple QWs [7,8], where the time evolution of the PL intensity associated with photogeneration of heavy holes was used to determine the local electron concentration. In this way, the influence of the external electric field on the heavy hole drift was studied. In the present work, we use photocurrent measurements to obtain the diffusion spatial distribution of holes injected into a QW. In this case, the different diffusion lengths of heavy and light holes allowed us to separate their contributions to the photocurrent. As a result, the different effects of an external electric field on light and heavy holes were found. Moreover, a QW depletion effect caused by the increase in the effective propagation length of holes with increasing electric field was discovered and shown to lead to different hole transport regimes.

The paper is organized as follows: Experimental details are given in Sec. II, qualitative analysis of the results is presented in Sec. III, a theoretical model is developed in Sec. IV, and the obtained results are discussed in Sec. V. Conclusions are given in Sec. VI.

II. EXPERIMENTAL

The sample used in this work was fabricated from a single GaAs QW, with a thickness of 14 nm, grown on a (100)-oriented GaAs substrate by a molecular beam epitaxy. QW barriers were grown in the form of short-period GaAs/AlAs superlattices. The sheet electron density and the mobility measured at the temperature of 1.4 K were 9.1×10^{11} cm^{-2} and 2.0×10^{6} cm^2 V^{-1} s^{-1}, respectively. In this structure, hydrodynamic electron transport in the form of viscous flow of electrons was demonstrated in Refs. [13,15–19] .

Scanning photocurrent microscopy experiments were performed using the potential probes of the multiterminal Hall bar structure with a width $W = 5$ μm and a length $L = 100$ μm of the active mesoscopic channel at the temperature of 3.7 K using a helium closed-cycle cryostat. An electrically connected sample was placed on top of an *x*-*y*-*z* nanopositioner stack (Attocube), which allows for precise positioning of the focused laser beam. The 440 nm (2.82 eV) illumination from the laser (Cobolt/08), whose energy is higher than the gap in the barriers, was focused onto the sample. The laser spot size is about 1 μm. During the measurements, the laser spot was scanned along the channel. The photocurrent measurements were carried out by a source meter Keithley 2400. The measurement scheme is given in detail in Ref. [13].

As will be explained in detail in the next section, the choice of excitation energy was determined by the conditions required to observe hole diffusion in the QW. More precisely, photogeneration of holes in an *n*-doped QW does not lead to the observation of their diffusion due to the very fast (within the Maxwellian relaxation time) response of background electrons, which tend to neutralize excess holes and thus maintain charge neutrality. At the same time, photogeneration of e-h pairs in barriers with their subsequent spatial separation by the built-in electric field leads to the injection of holes into the QW and the accumulation of electrons in the barriers. As a result, no electric field arises in the QW plane that can force background electrons to neutralize the injected holes, while diffusion returns the e-h system to the equilibrium.

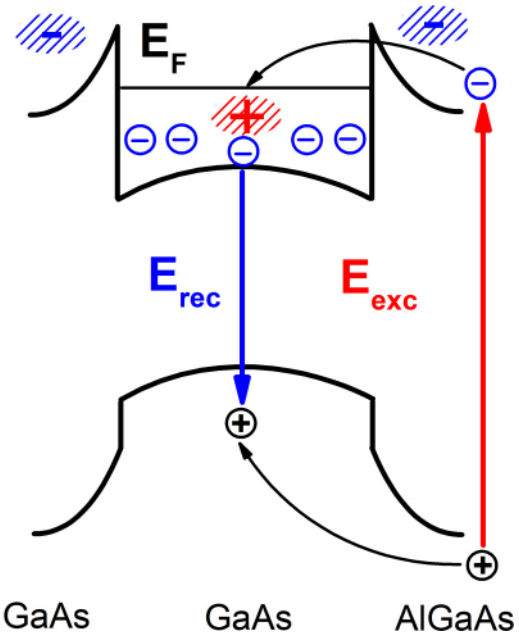

FIG. 1. Schematic diagram of the formation of a positive space charge (shown as the shaded red region) in a QW. Electrons accumulated in the barriers near the heterointerface form a negative space charge (shown as the shaded blue region) that balances the positive space charge in the QW.

In addition, the recombination time was measured by time-resolved PL with a temporal resolution of 100 ps using the PicoQuant/LDH Series diode lasers emitting 80 MHz pulses with a pulse duration of 70 ps. The PL decay transients were detected by a PicoQuant Hybrid PMT detector triggered with a time-correlated single-photon PicoQuant/PicoHarp 300 counting system.

III. RESULTS

In the studied doped QW, no photocurrent was detected when exposed to illumination with energy above the QW band gap but below the barrier band gap [18]. This is consistent with the fact that the photoelectric effect is not expected in highly conductive materials, where space charge is not generated within realistic observation times due to Maxwell relaxation. At the same time, when photoexcited by light whose energy exceeds the gap in the barriers, a photocurrent is observed. This photocurrent arises from the optical depletion effect, first discovered in highly doped GaAs/AlGaAs QW by Chaves *et al.* [20], which results in the formation of a positive space charge in the QW. The scheme of optical excitation and formation of a positive space charge in a QW is shown in Fig. 1. The built-in electric field of the heterointerface separates electrons and holes photogenerated in the barriers: Holes are injected into the QW, recombine with background electrons and thereby create a space positive charge there due to the uncompensated charge of ionized impurities, and

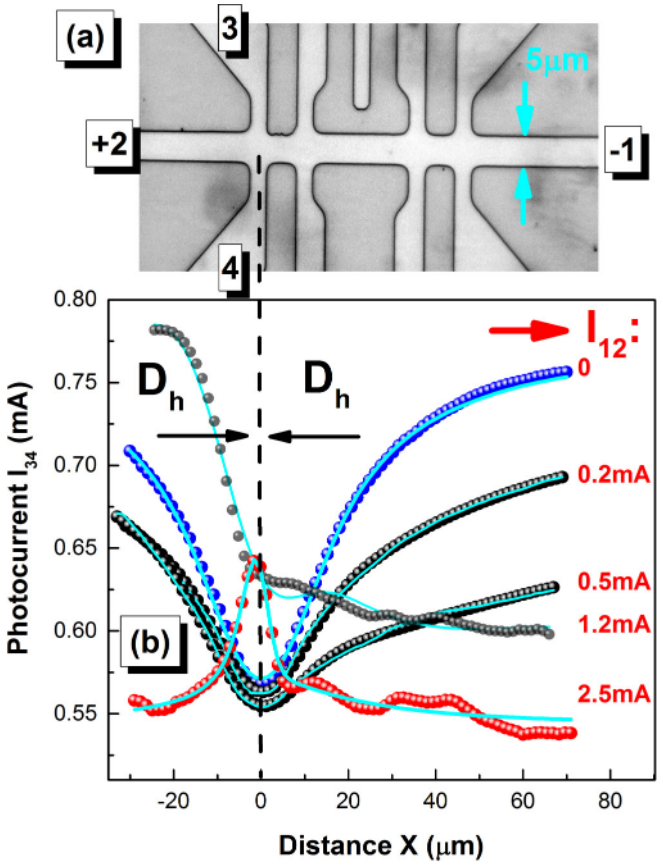

FIG. 2. (a) Microscope image of the sample. (b) Photocurrent I_{34} (circles) measured at $T = 3.7$ K between collecting probes 3 and 4 at different electric currents I_{12} through probes 1 and 2. The cyan lines represent calculated spatial diffusion profiles. Black and red arrows indicate the directions of hole diffusion and electric current, respectively.

photoexcited electrons accumulate in barriers near the heterointerface. The positive charge induced in the QW lowers the potential barrier for electrons and thus promotes their injection from the barriers into the QW, compensating for the loss of background electrons. Finally, in the stationary case, a positive space charge is formed in the QW on the scale of the diffusion length of the injected holes and is determined by the balance between holes and electrons transferred into the QW from the barrier. The spatial distribution of this positive charge is then measured using microphotocurrent equipment as described below.

It is important to note that in the region of photogeneration, the electroneutrality of the e-h system under study is ensured by the negative charge of the electrons accumulated in the barriers. Thus, the electric field is not related to the spatial distribution of holes in the QW plane, the latter distribution is therefore due to diffusion.

In general terms, the processes of formation of a positive charge and the corresponding depletion of the QW were considered in Refs. [20–22]. However, the processes that determine the spatial distribution of the positive charge induced in the QW are still unclear.

A microscopic image of the sample is shown in Fig. 2(a). A constant electric field applied to collecting probes 3 and 4 leads to a corresponding dc electric current I_{34}. Laser excitation causes injection of holes from the barriers into the channel. The injected holes diffuse from the laser spot to collecting probes 3 and 4, where they recombine with the background electrons, reducing the current I_{34}. This current, measured as a function of the distance x between the laser spot and the collection probes, reproduces the spatial diffusion profile of the holes. In addition, a constant electric field applied to the ends of the channel (probes 1 and 2) causes a dc electric current I_{12} to flow through the channel. The spatial diffusion profiles measured along the channel at different currents I_{12} in the channel are shown in Fig. 2(b). Raw experimental data are available in Ref. [23].

In the absence of current I_{12} in the channel, the spatial diffusion profile is represented by a shape of the photocurrent I_{34} minimum, symmetrical with respect to collecting probes 3 and 4. As the current increases, the diffusion profile becomes asymmetric, indicating an increase in the propagation length of holes λ in the direction opposite to the current, i.e., in the direction of electron flow. Obviously, the observed asymmetry of the diffusion profile is due to the entrainment of holes by electrons. To our knowledge, the first observation of asymmetric diffusion of different ions under electric field was presented by Arnikar [24], while the asymmetry of diffusion profiles similar to that shown in Fig. 2(b), measured using spatially resolved PL in multiple p-doped GaAs/AlGaAs quantum wells, was shown to arise due to the e-h Coulomb drag [7,8].

It is significant that in the case of one type of holes, the drag is expected to increase the width of the spatial diffusion profile on the side where the holes diffuse in the direction of the electron flow (to the right of the minimum), whereas on the opposite side, where holes diffuse against electrons, the width of the diffusion profile should decrease. However, no significant reduction in the width of the diffusion profile to the left of the minimum was detected. It will be shown below that this is due to the diffusion of two types of holes: heavy and light, which diffuse in opposite directions. Moreover, unexpectedly, at a high current I_{12} in the channel, an inverted shape of the spatial diffusion profile with a maximum at the collecting contacts was discovered.

It is worth mentioning that the observed increase in the hole propagation length λ with increasing current I_{12} can lead to depletion of the entire channel when the propagation length exceeds the channel length L.

When an external electric field E_{34} is applied to the probes 3 and 4, the photocurrent density is determined as $j_{34} = \sigma E_{34}$ with conductivity

$$\sigma(x) = e[n_0 - p(x)]\mu_e + en_c(x)\mu_e^* + ep_c(x)\mu_p^*, \quad (1)$$

where e is the electron charge, n_0 and μ_e are the concentration and mobility of background electrons, respectively, p is the concentration of the injected holes, $n_c = p_c$ are the concentrations of electrons and holes photogenerated inside the QW, and $\mu_e^* \simeq \mu_p^*$ are their ambipolar mobilities.

When the first term dominates, optical depletion and corresponding minimum photocurrent occur. This is expected when $\mu_e \gg \mu_e^*, \mu_p^*$. While in an entirely depleted channel at $p \simeq n_0$,

the conductivity becomes $\sigma(x) \simeq en_c(x)\mu_e^* + ep_c(x)\mu_p^*$. Thus, in a depleted channel, the photocurrent is driven by e-h pairs photogenerated within the QW. Reaching collection probes 3 and 4, these e-h pairs directly contribute to the photocurrent, resulting in a maximum of spatial diffusion profile.

In this way, Eq. (1) reflects two transport regimes that can be realized in a QW under photoexcitation conditions: (1) $\lambda < L$, when the channel conductivity is due to background electrons, and (2) $\lambda > L$, when ambipolar diffusion dominates.

To explain the observed phenomenon, we have developed a theory of Coulomb drag in our case, when holes are injected into a hydrodynamic electron system, based on the standard drift-diffusion approximation, which is given in the next section.

IV. THEORETICAL MODEL

The linear response of the e-h plasma studied here was confirmed in Ref. [12], which proves the use of the standard drift-diffusion approach. In the case considered here, the continuity equations have the form

$$\frac{\partial n}{\partial t} + \mathrm{div}(\mathbf{j}_e/e) + \gamma np = \frac{n - n_0}{\tau_o}, \tag{2a}$$

$$\frac{\partial p}{\partial t} - \mathrm{div}(\mathbf{j}_h/e) + \gamma np = G_p, \tag{2b}$$

where n and p are the electron and hole densities in the sample, coefficient γ describes the e-h recombination, $\mathbf{j}_e$ and $\mathbf{j}_h$ are the electron and hole electric currents, respectively, and $e = -|e|$ is the electron charge. The right-hand side of the hole continuity equation contains G_p, generation rate of the holes in the channel at the above-barrier illumination as described in Sec. III and Fig. 1. The right-hand side of the electron continuity equation contains the term that describes slow relaxation of electron density n toward its equilibrium (background) value n_0 related to the doping and τ_o is a recharging time of the structure.

The electric current densities of the charge carriers can be expressed in a standard way:

$$\mathbf{j}_e = -eD_e\nabla n + \sigma_e\mathbf{E} - \frac{\mathbf{j}_e + \frac{n}{p}\mathbf{j}_h}{\tau_{eh}/\tau_e} = \sigma_e\mathbf{E}_e - \frac{\mathbf{j}_e + \frac{n}{p}\mathbf{j}_h}{\tau_{eh}/\tau_e}, \tag{3a}$$

$$\mathbf{j}_h = +eD_h\nabla p + \sigma_h\mathbf{E} - \frac{\mathbf{j}_h + \frac{p}{n}\mathbf{j}_e}{\tau_{eh}/\tau_e} = \sigma_h\mathbf{E}_h - \frac{\mathbf{j}_h + \frac{p}{n}\mathbf{j}_e}{\tau_{eh}/\tau_e}, \tag{3b}$$

where $D_{e,h}$ are the electron and hole diffusion coefficients and $\sigma_{e,h} = n_{e,h}e^2\tau_{e,h}/m_{e,h}$ are their conductivities, with $n_e = n$ and $n_h = p$, $\tau_{e,h}$ are the electron and hole momentum relaxation times, and $m_{e,h}$ are their effective masses. In Eq. (3), τ_{eh} is the e-h scattering time. Accordingly, the last terms describe the e-h drag. The generalized fields $\mathbf{E}_e = \mathbf{E} - \frac{1}{e}\nabla\mu_e$ and $\mathbf{E}_h = \mathbf{E} - \frac{1}{e}\nabla\mu_h$ take into account the chemical potential ($\mu_{e,h}$) gradients, and we used the Einstein relation to interrelate the diffusion coefficients and conductivities.

These equations follow from simplified microscopic equations for the ensemble average electron and hole velocities $\mathbf{v}_{e,h} = 2\sum_{\mathbf{k}}(\hbar\mathbf{k}/m_{e,h})f_{e,h}(\mathbf{k})$, where the factor 2 takes into account the spin degeneracy of the charge carriers and $f_{e,h}(\mathbf{k})$ are the distribution functions of electrons and holes:

$$\frac{\partial \mathbf{v}_e}{\partial t} + \frac{\mathbf{v}_e}{\tau_e} + \frac{\mathbf{v}_e - \mathbf{v}_h}{\tau_{eh}} = \frac{e\mathbf{E}_e}{m_e}, \tag{4a}$$

$$\frac{\partial \mathbf{v}_h}{\partial t} + \frac{\mathbf{v}_h}{\tau_h} + \frac{\mathbf{v}_h - \mathbf{v}_e}{\tau_{eh}} = \frac{-e\mathbf{E}_e}{m_h}. \tag{4b}$$

In Eqs. (2) and (3), the generation and recombination terms are omitted because these processes typically occur on much longer timescales compared to the microscopic scales of the momentum and interparticle scattering. For the same reason, terms with $\partial//\partial t$ are disregarded. Hence, Eq. (4) can be solved in the steady-state conditions, and taking into account that $\mathbf{j}_{e,h} = en\mathbf{v}_{e,h}$, we arrive at Eq. (3).

Equations (3) and (4) are derived in the diffusive regime under the assumption that the momentum of the particles is lost due to the scattering in the bulk of the channel. In the viscous hydrodynamic regime, it may not be the case: The momentum of the quasiparticles is dissipated by the scattering at the channel edges, while the viscosity enables the transfer of momentum from "fast" quasiparticles in the middle of the channel to the "slow" quasiparticles near the edges. In that case, τ_e and τ_h in Eq. (3) should be considered as phenomenological parameters that take into account the viscosity and control the conductivities of the electrons and holes.

According to Ref. [25], these phenomenological effective scattering times can be recast as $\tau_i = \tau_{pi} \cdot \tau_i^*/(\tau_{pi} + \tau_i^*)$, where $i = e$ or h, τ_{pi} is the momentum relaxation time in the channel bulk, and $\tau_i^* = w^2/12\eta$ is the viscosity-related contribution, with η and w being the effective viscosity of the carriers and the channel width, respectively. Similarly, effective electron-hole scattering time τ_{eh} can contain contribution due to the drag viscosity [10].

As discussed above, photoinjection of holes into a quantum well results in the formation of a positive space charge accompanied by a corresponding electric field. In such a case, the electric field $\mathbf{E}$ should be found self-consistently taking into account both the external field and the fields produced by separation of electrons and holes in the QW plane. It satisfies the Poisson equation (with appropriate boundary conditions)

$$\mathrm{div}(\epsilon\mathbf{E}) = 4\pi(n - p)\delta(z), \tag{5}$$

where ϵ is the permittivity of the medium and the $\delta(z)$ function with z being the direction normal to the QW plane takes into account the fact that electrons and holes are in a two-dimensional layer. In two-dimensional systems, this field produces rapid neutralization of the system [14,26]. In our case, we assume that the additional positive charge in the QW is compensated by the negative charge of electrons in the barriers; therefore, total charge does not appear. Hence, for simplicity, we consider a model where the electric field of the space charge is disregarded. Thus, we can consider drift and diffusion of holes only assuming a given dc current of electrons. Furthermore, under assumption of $n \gg p$, the continuity equation becomes

$$\frac{p}{T_p} = D_h\frac{d^2}{dx^2}p - V_h\frac{d}{dx}p + G_p. \tag{6}$$

Here, $T_p = 1/(\gamma n)$ is the recombination time of holes and V_h is the effective drift velocity of the holes (resulting from both the external field and e-h collisions). The velocity contains two components due to (1) hole drift in the field $\mathbf{E}$ and (2) hole drag by the electrons, and can be recast as

$$\mathbf{V}_h = \mu_h \mathbf{E} - \mu_e \frac{\tau_h}{\tau_h + \tau_{eh}} \mathbf{E}, \tag{7}$$

where $\mu_{e,h} = |e|\tau_{e,h}/m_{e,h} > 0$ is the hole (electron) mobility, and we recall that $\mathbf{E}$ is the component of electric field along the channel. Here, we assume that the electron drift in the field is unaffected by the e-h scattering. The effective velocity $\mathbf{V}_h \neq 0$ is responsible for the asymmetry of the spatial diffusion profile of holes. The diffusion profile is symmetric when $\mathbf{V}_h = 0$, while a finite value of the effective velocity results in diffusion asymmetry: due to drift or drag when $V_h > 0$ or $V_h < 0$, respectively.

The linear equation (5) can be readily solved by the Green's function method. We introduce

$$g(x, x') = \sqrt{\frac{T_p}{D_h^*}} \times \exp\left[-\frac{\sqrt{D_h^*}}{2D_h T_p^{1/2}} |x' - x| - \frac{V_h}{2D_h}(x' - x) \right] \tag{8}$$

where $D_h^* = 4D_h + T_p V_h^2$ is the effective diffusion coefficient of holes; hence, the steady-state solution of the drift-diffusion equation is represented as

$$p(x) = \int_{-\infty}^{\infty} g(x, x') G_p(x') dx'. \tag{9}$$

For a Gaussian profile of the excitation,

$$G_p(x) = G_o \exp\left(-\frac{x^2}{\sigma^2} \right), \tag{10}$$

where σ characterizes the dispersion and G_o is the prefactor determined by the above-barrier illumination. As a result, we can evaluate the steady-state spatial profile of holes as

$$p(x) = G_o \frac{\sqrt{\pi}\sigma}{2} \sqrt{\frac{T_p}{D_h^*}} \times \exp\left[\frac{(V_h\sigma^2 + 4D_h x)\lambda_- + 2D_h\sigma^2}{8D_h^2 T_p} \right] \times \left\{ 1 + \operatorname{erf}\left(\frac{x}{\sigma} + \frac{\lambda_- \sigma}{4D_h T_p} \right) + \exp\left[\frac{\sqrt{\frac{4D_h}{T_p} + V_h^2}(V_h\sigma^2 + 4D_h x)}{4D_h^2} \right] \times \operatorname{erf}\left(\frac{x}{\sigma} + \frac{\lambda_+ \sigma}{4D_h T_p} \right) \right\}. \tag{11}$$

In Eq. (11), $\lambda_\pm = V_h T_p \pm \sqrt{T_p(4D_h + V_h^2 T_p)}$ are the effective propagation length in the direction of ($\lambda_+ > 0$) and against ($\lambda_- < 0$) the velocity V_h. In the purely diffusive case ($V_h = 0$), $\lambda_\pm = \pm 2\sqrt{T_p D_h}$ and $|\lambda_\pm|$ is twice the diffusion length. In the presence of drift and drag, $V_h \neq 0$ and $V_h T_p \gg \sqrt{4T_p D_h}$. In this case, $\lambda_+ \simeq +V_h T_p$ determines the effective propagation length along V_h over the lifetime of the hole, while $\lambda_- \simeq -2D_h/V_h$ describes the tail of the hole profile in the direction opposite to V_h.

As shown in Ref. [13], in the studied sample, the two hole species are present: heavy and light holes. Therefore, at high injection level, the electron concentration responsible for the diffusion profile of the photocurrent is $n(x) = n_0 - p(x)$, where $p(x) = p_{hh}(x) + p_{lh}(x)$ are the concentrations of heavy (hh) and light (lh) holes injected into the channel from the barriers, which recombine with background electrons. Thus, the hole spatial diffusion profile consists of two corresponding contributions, each of which is calculated according to Eq. (11). In contrast, in the entirely depleted channel, $n(x) = n_0^* + n_{ch}(x) + p_{ch}(x)$, where n_0^* is the residual concentration of background electrons, and the concentrations of electrons and holes as a function of distance x are calculated according to Eq. (11).

In general, spatial diffusion profiles are determined by numerous parameters related to heavy and light holes photogenerated in the QW and injected from the barriers. The parameters that most influence the shape of the spatial diffusion profile are the effective drift velocities V_h and the recombination times T_p, determined for both light and heavy holes. Furthermore, the contributions of heavy and light holes are spatially separated due to their different diffusion lengths. Heavy holes influence the diffusion profile near the collecting contacts, while the influence of light holes is pronounced at larger distances. In addition, the contributions of holes photogenerated in the QW and injected from the barriers affect the photocurrent differently. At low electric current in the channel, the contribution of holes injected from the barriers predominates, which leads to a minimum of the spatial diffusion profile. However, as discussed in the next section, at high channel current the maximum of the diffusion profile is entirely due to holes photogenerated inside the QW.

Thus, despite the many parameters, fitting experimental spatial diffusion profiles results in a unique set of parameters.

V. DISCUSSION

First, a symmetric spatial diffusion profile ($V_h = 0$), measured without current, with contributions from light and heavy holes only, was fitted to obtain the diffusion coefficients of light and heavy holes $D_{lh} = 0.81\,\mathrm{m^2\,s^{-1}}$ and $D_{hh} = 0.04\,\mathrm{m^2\,s^{-1}}$, respectively. The obtained heavy hole diffusion coefficient was then used to fit the spatial diffusion profile measured in the depleted channel at $I_{12} = 2.5$ mA, when ambipolar diffusion of electrons and heavy holes photogenerated in the channel was observed. The electron diffusion coefficient obtained in this way $D_e = 0.66\,\mathrm{m^2\,s^{-1}}$ agrees with the electron diffusion coefficient $D_e = 1.1\,\mathrm{m^2\,s^{-1}}$ obtained in the same structure in Ref. [27] using magnetotransport measurement data. These diffusion coefficients were then used to fit diffusion profiles measured at different channel currents.

With increasing current I_{12}, the increase in the electron drift velocity leads to an increase in the propagation length of holes in the direction of the electron flow ($x > 0$), which occurs due to Coulomb drag. When the propagation length

of holes becomes greater than the channel length, diffusion no longer determines the flow of holes in the channel. In this case, observed at $I_{12} = 2.5$ mA, the low photocurrent I_{34} indicates entire channel depletion due to recombination of background electrons with injected holes and the photocurrent is expected to become distance independent. Instead, a maximum of the photocurrent is found. The observed maximum of photocurrent is a manifestation of the ambipolar diffusion of electron-hole pairs photogenerated inside the QW, rather than holes injected from the barriers.

The best-fit results for the experimental spatial diffusion profiles are shown in Fig. 2(b), which demonstrate good agreement with the theory. Apparently, in the depleted channel where diffusion is insignificant, the drift of holes should determine their flow in an external electric field. Indeed, the asymmetry of the corresponding diffusion profile measured at $I_{12} = 2.5$ mA indicates an increase in the diffusion length of holes that propagate in the direction of the electric field ($x < 0$), which corresponds to a dominant drift regime.

Thus, depending on the current in the channel, two hole transport regimes are observed: diffusion and drift at low and high currents, respectively. In addition, in the diffusion regime, the Coulomb e-h drag strongly influences the hole diffusion.

The best fits of the spatial diffusion profiles were obtained as a superposition of the profiles shown in Fig. 3, for the selected diffusion profiles.

The diffusion profiles shown in Figs. 3(a) and 3(b) represent the minima due to dominating contribution of heavy and light holes injected from the barriers. Although the density of heavy holes photogenerated in barriers is expected to be higher than that of light holes, the presented results show that the concentration of light holes injected into the QW is higher than that of heavy holes. This is due to the fact that, according to the Wentzel-Kramers-Brillouin approximation [28], the probability of tunneling through a heterointerface is proportional to $\exp(-2\frac{\sqrt{2mE}}{\hbar}x)$, where m and E are the mass and energy of the particle, respectively, and x is the tunneling distance. Consequently, the injection rate of light holes is higher than that of heavy holes. Thus, the heterointerface acts as a filter, allowing more light holes to pass through and blocking heavy holes.

An increase in the current I_{12} leads to channel depletion. In this case, the ambipolar diffusion of electron-heavy hole pairs photogenerated in the QW begins to play a notable role, and the corresponding maximum of the diffusion profile is detected at $I_{12} = 0.8$ mA, shown in Fig. 3(c). The asymmetry of this maximum indicates a predominant electron drift. As I_{12} increases further, ambipolar diffusion becomes dominant and the maximum of the diffusion profile consisting of electron and heavy hole contributions is observed in Fig. 3(d). In such a case, the profile shapes of both electrons and holes exhibit a drift in the external electric field. This demonstrates the effect of the electric field on ambipolar diffusion: The propagation length of holes increases in the direction of the field/current, while the propagation length of electrons increases in the opposite direction.

The characteristic parameters of the studied e-h system, obtained as a result of fitting the spatial diffusion profiles, are presented in Fig. 4.

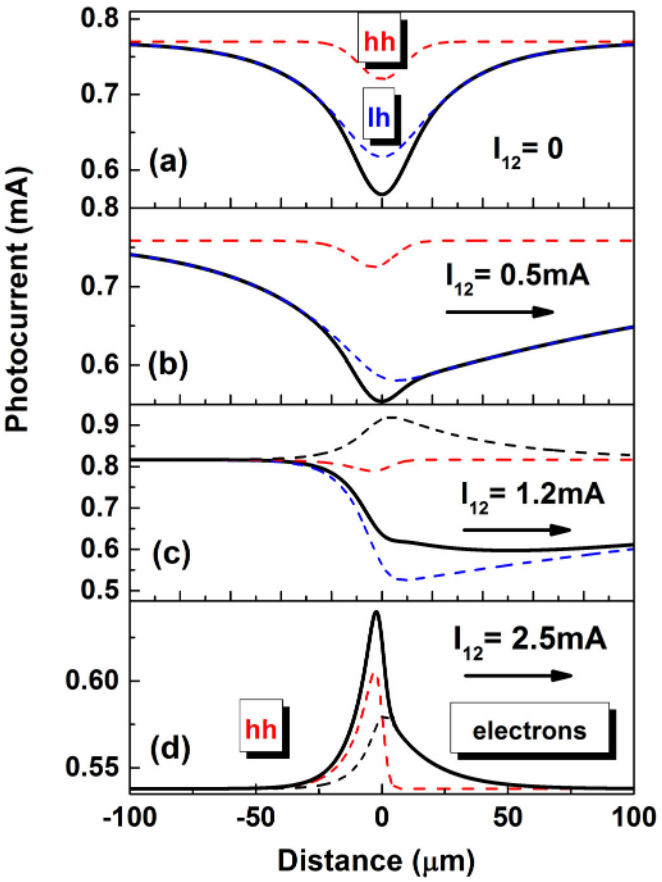

FIG. 3. Fits of spatial diffusion profiles from Fig. 2(b) calculated for different channel currents I_{12}. For each diffusion profile (solid black lines), the contributions of light (blue dashed lines) and heavy (red dashed lines) holes and electrons (black dashed lines) are shown. The arrows show the direction of the current I_{12}.

The effective drift velocities are shown in Fig. 4(a). The external electric field causes counterflows of heavy and light holes: Heavy holes propagate in the direction of the electric field ($V_{hh} > 0$). This means that the first term in Eq. (7), responsible for the hole drift, dominates. At the same time, light holes propagate in the direction opposite to the electric field ($V_{hh} < 0$), in the same direction as the electrons ($V_e < 0$), which is due to the dominant second term in Eq. (7), responsible for the e-h Coulomb drag. As follows from Eq. (7), in the hydrodynamic e-h plasma, where momentum-conserving e-h scattering dominates momentum-relaxing scattering of holes ($\tau_h \gg \tau_{eh}$), a negative effective hole drift velocity is expected when the electron and hole mobilities are related as $\mu_e > \mu_h$.

According to the model presented in Sec. IV, the resulting asymmetry of the spatial diffusion profile is determined by the relation between the effective propagation lengths in the direction of the electric field (λ_+) and against it (λ_-). Dominant λ_+ or λ_- indicates drift of holes or their electron drag, respectively. A corresponding dominance is determined by the total effective propagation length ($\lambda_+ + \lambda_-$), where $\lambda_+ > 0$ and $\lambda_- < 0$. Accordingly, a positive or negative total effective propagation length ($\lambda_+ + \lambda_-$) indicates drift or drag regimes, respectively.

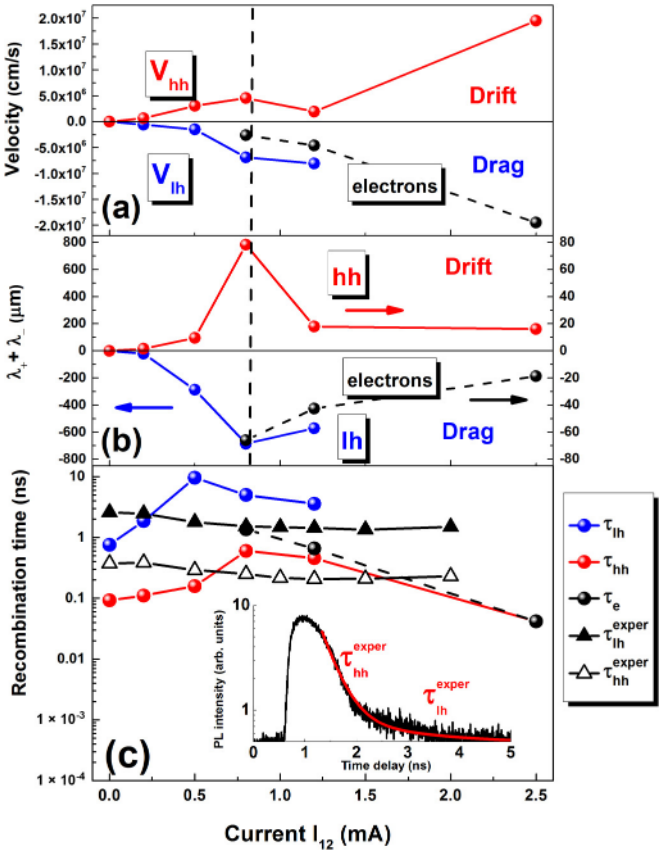

FIG. 4. (a) Effective drift velocity, (b) total effective propagation length ($\lambda_+ + \lambda_-$), and (c) recombination time of light and heavy holes and electrons in a biased channel obtained by fitting the corresponding spatial diffusion profiles shown in Fig. 2(b). The vertical dashed line separates the diffusion (on the left) and drift (on the right) regions. Positive and negative effective drift velocities and total effective propagation length correspond to drift and drag transport regimes, respectively. Inset in panel (c) shows the PL transient measured at $T = 3.7$ K and $I_{12} = 0.5$ mA together with the best fit, while the experimental heavy and light hole recombination times measured as a function of current are shown as black dots in panel (c).

The total effective propagation lengths ($\lambda_+ + \lambda_-$) shown in Fig. 4(b) reveal a behavior similar to the effective velocities, consistent with the drift of heavy holes and the drag of light holes. In the diffusion regime, the drift of heavy holes and the drag of light holes lead to an increase in the total effective propagation lengths associated with them with increasing current in the channel. With further increase in current, the total effective propagation length of heavy holes decreases due to the enhancement of electron-phonon scattering caused by the current-induced heating of electrons [12]. The presented results show that in the studied sample the electron-light hole scattering is stronger than the electron-heavy hole scattering. As a result, negative conductivity of light holes due to the Coulomb e-h drag is observed.

The above analysis is based on a comparison of the experimental spatial diffusion profiles with those calculated according to the model presented in Sec. IV, which predicts an exponential profile for the diffusion of one type of holes. The deviation from the expected shape of the diffusion profile is attributed to the contribution of additional carriers. The simplest cases correspond to the spatial diffusion profile measured in an unbiased channel (without current) and the profile measured in a depleted channel. In both cases, two dominant carrier types were found: heavy and light holes and heavy holes and electrons in the unbiased and depleted channels, respectively. In addition, in the intermediate case, a clear contribution of electrons photogenerated in the channel was observed.

Furthermore, PL decay transients were measured at the emission maxima. As shown in the inset of Fig. 4(c), they exhibit a biexponential decay with characteristic times of light and heavy holes. The experimental recombination times obtained by fitting the PL transients are shown in Fig. 4(c) together with the light and heavy hole recombination times obtained by fitting the measured spatial diffusion profiles. The reasonable agreement between the measured heavy hole recombination time and the time obtained by fitting the diffusion profiles proves the correctness of the model used.

VI. SUMMARY

The transport of holes optically injected into a mesoscopic GaAs channel, where electrons exhibit hydrodynamic properties, has been studied. Two types of diffusion are observed: (1) diffusion of holes injected from barriers in the background electron environment and (2) ambipolar diffusion of electron-hole pairs photogenerated inside the channel. Ambipolar diffusion is not visible in the presence of high background electron concentration. In this case, diffusion of holes injected from barriers dominates. The injected holes cause channel depletion on the scale of their diffusion length. An external electric field applied to the channel leads to an increase in the propagation length of holes. It was found that the effective propagation length of heavy holes increases due to their drift, while the increase in the effective propagation length of light holes is due to their Coulomb drag by electrons. As a result of the different actions of an external electric field on light and heavy holes, a remarkable effect was discovered in which an external electric field causes counterflows of heavy and light holes: Heavy holes propagate in the direction of the electric field, while Coulomb drag causes light holes to move in the direction opposite to the electric field, the same direction as the electrons. As a consequence of the Coulomb e-h drag, negative conductivity of light holes is observed. Moreover, an increase in the effective propagation length of holes leads to a change in their transport mode from diffusion to drift, as well as to channel depletion when the propagation length exceeds the channel length. In this case, ambipolar diffusion of electron-hole pairs photogenerated inside the channel is manifested. A theoretical model of the Coulomb drag of holes by electrons is developed, which made it possible to determine the characteristic parameters of the hydrodynamic electron-hole system such as diffusion coefficients, effective drift velocities, recombination times, and effective diffusion lengths of light and heavy holes. The theory explains well the obtained experimental results and demonstrates that the basic physics of electron-hole drag can be easily captured using the simple drift-diffusion model.

ACKNOWLEDGMENTS

Financial support from the Brazilian agency FAPESP (Grants No. 2021/12470-8 and No. 2022/10340-2) is gratefully acknowledged. M.M.G. is grateful to RSF Grant No. 22-12-00211-Continuation (analytical model).

DATA AVAILABILITY

The data that support the findings of this article are openly available [23], embargo periods may apply.

[1] L. Fritz and T. Scaffidi, Hydrodynamic electronic transport, Annu. Rev. Condens. Matter Phys. **15**, 17 (2024).

[2] P. M. Solomon, P. J. Price, D. J. Frank, and D. C. La Tulipe, New phenomena in coupled transport between 2D and 3D electron-gas layers, Phys. Rev. Lett. **63**, 2508 (1989).

[3] T. J. Gramila, J. P. Eisenstein, A. H. MacDonald, L. N. Pfeiffer, and K. W. West, Mutual friction between parallel two-dimensional electron systems, Phys. Rev. Lett. **66**, 1216 (1991).

[4] B. N. Narozhny and A. Levchenko, Coulomb drag, Rev. Mod. Phys. **88**, 025003 (2016).

[5] T. P. McLean and E. G. S. Paige, Electron-hole scattering and minority carrier mobility in germanium, J. Phys. Chem. Solids **18**, 139 (1961).

[6] M. Marohashi, N. Sawaki, and I. Akasaki, Electron mobility and drag effect in p-type silicon, Jpn. J. Appl. Phys. **24**, 732 (1985).

[7] R. A. Hopfel, J. Shah, P. A. Wolff, and A. C. Gossard, Negative absolute mobility of minority electrons in GaAs quantum wells, Phys. Rev. Lett. **56**, 2736 (1986).

[8] R. A. Hopfel, J. Shah, P. A. Wolff, and A. C. Gossard, Electron-hole scattering in GaAs quantum wells, Phys. Rev. B **37**, 6941 (1988).

[9] L. A. Ponomarenko, A. Principi, A. D. Niblett, W. Wang, R. V. Gorbachev, P. Kumaravadivel, A. I. Berdyugin, A. V. Ermakov, S. Slizovskiy, K. Watanabe, T. Taniguchi, Q. Ge, V. I. Fal'ko, L. Eaves, M. T. Greenaway, and A. K. Geim, Extreme electron–hole drag and negative mobility in the Dirac plasma of graphene, Nat. Commun. **15**, 9869 (2024).

[10] E. H. Hasdeo, E. G. Idrisov, and T. L. Schmidt, Coulomb drag of viscous electron fluids: Drag viscosity and negative drag conductivity, Phys. Rev. B **107**, L121107 (2023).

[11] D. Svintsov, V. Vyurkov, S. Yurchenko, T. Otsuji, and V. Ryzhii, Hydrodynamic model for electron-hole plasma in graphene, J. Appl. Phys. **111**, 083715 (2012).

[12] Y. A. Pusep, M. A. T. Patricio, G. M. Jacobsen, M. D. Teodoro, G. M. Gusev, and A. K. Bakarov, Current-induced magnetoexcitons in mesoscopic electron-hole plasma, arXiv:2507.19678.

[13] Y. A. Pusep, M. D. Teodoro, V. Laurindo, Jr., E. R. C. de Oliveira, G. M. Gusev, and A. K. Bakarov, Diffusion of photoexcited holes in a viscous electron fluid, Phys. Rev. Lett. **128**, 136801 (2022).

[14] M. I. D'yakonov and A. S. Furman, Charge relaxation in an anisotropic medium and in low-dimensional media, Sov. Phys. JETP **65**, 574 (1987).

[15] G. M. Gusev, A. D. Levin, E. V. Levinson, and A. K. Bakarov, Viscous electron flow in mesoscopic two-dimensional electron gas, AIP Adv. **8**, 025318 (2018).

[16] A. D. Levin, G. M. Gusev, E. V. Levinson, Z. D. Kwon, and A. K. Bakarov, Vorticity-induced negative nonlocal resistance in a viscous two-dimensional electron system, Phys. Rev. B **97**, 245308 (2018).

[17] G. M. Gusev, A. D. Levin, E. V. Levinson, and A. K. Bakarov, Viscous transport and Hall viscosity in a two-dimensional electron system, Phys. Rev. B **98**, 161303(R) (2018).

[18] Yu A. Pusep, M. D. Teodoro, M. A. T. Patricio, G. M. Jacobsen, G. M. Gusev, A. D. Levin, and A. K. Bakarov, Dynamics of recombination in viscous electron–hole plasma in a mesoscopic GaAs channel, J. Phys. D: Appl. Phys. **56**, 175301 (2023).

[19] M. A. T. Patricio, G. Jacobsen, M. D. Teodoro, G. M. Gusev, A. K. Bakarov, and Y. A Pusep, Hydrodynamics of electron-hole fluid photogenerated in a mesoscopic two-dimensional channel, Phys. Rev. B **109**, L121401 (2024).

[20] A. S. Chaves, A. F. S. Penna, J. M. Worlock, G. Weimann, and W. Schlapp, Optical control of two-dimensional electron density in a single asymmetric quantum well, Surf. Sci. **170**, 618 (1986).

[21] D. Richards, G. Fasol, and K. Ploog, Raman scattering verification of nonpersistent optical control of electron density in a heterojunction, Appl. Phys. Lett. **57**, 1099 (1990).

[22] M. Hayne, A. Usher, A. S. Plaut, and K. Ploog, Optically induced density depletion of the two-dimensional electron system in GaAs/AlGaAs heterojunctions, Phys. Rev. B **50**, 17208 (1994).

[23] Y. A. Pusep, Data set: Photocurrent I_{34} profiles at different drag voltages V12, (2025), https://pastebin.com/T9aV2Rvp.

[24] H. J. Arnikar, An anisotropy effect in diffusion under electric field, Nature (London) **194**, 271 (1962).

[25] P. S. Alekseev. Negative magnetoresistance in viscous flow of two-dimensional electrons, Phys. Rev. Lett. **117**, 166601 (2016).

[26] V. I. Fal'ko and D. E. Khmel'nitskii, What if the film conductivity is higher than the speed of light? J. Exp. Theor. Phys. **68**, 1150 (1989).

[27] A. D. Levin, G. M. Gusev, V. A. Chitta, Z. D. Kvon, A. S. Jaroshevich, D. E. Utkin, D. V. Dmitriev, and A. K. Bakarov, Obstacle-induced Gurzhi effect and hydrodynamic electron flow in two-dimensional systems, Phys. Rev. B **111**, 125302 (2025).

[28] C. Kittel, *Introduction to Solid State Physics*, 8th ed. (John Wiley & Sons, Inc., 2005).